G. Etse
e-mail: getse@herrera.unt.edu.ar

S. M. Vrech

Centro de Métodos Numéricos y Computacionales en Ingeniería,
University of Tucuman,
Muñecas 730,
10A, 4000 Tucumán,
Argentina

Geometry Method for Localization Analysis in Gradient-Dependent J_2 Plasticity

In this work the geometrical method for the assessment of discontinuous bifurcation conditions is extended to encompass gradient-dependent plasticity. To this end, the gradient-dependent localization condition is cast in the form of an elliptical envelope condition in the coordinates of Mohr. The results in this work demonstrate the capability of thermodynamically consistent gradient-dependent elastoplastic model formulations to suppress the localized failure modes of the classical plasticity that take place when the hardening/softening modulus $\bar{H}$ equals the critical value for localization $\bar{H}_c$, provided the characteristic length l remains positive. [DOI: 10.1115/1.2202348]

1 Introduction

Finite element solutions of boundary value problems involving strain-softening materials are strongly affected by mesh-dependency when the governing equations turn ill-posed. This is related to the formation of spatial discontinuities of kinematic fields and consequently, to a discontinuous bifurcation condition, see among others, Nadai [1], Thomas [2], Hill [3], and Rudnicki and Rice [4]. To reduce the loss of objectivity of the related computational results, two strategies are at hand: to improve the finite element technology or to regularize the description of the material behavior at the constitutive level.

To solve the mesh sensitivity of the computational predictions of strain softening material models, two possible strategies are at hand. On one hand, to improve the finite element technology by developing both standard finite element formulations, which are able to follow the post-bifurcation localization using realignment methods, and enhanced finite elements with discontinuous interpolation capabilities. On the other hand, to regularize the description of the material behavior at the constitutive level. However, a combination of both approaches seems to be the most effective one.

The regularization strategy leads to enriched material formulations that are mostly based on nonlocal approaches. Thereby, the gradients of the displacement function are evaluated in the vicinity of the material point, thus a spatial average is taken into account to evaluate the point value. This is accomplished by defining suitable weighted averages (nonlocal formulations) or gradients (gradient formulations) of a selection of thermodynamic variables.

In the literature, gradient-dependent material theories have been advocated within two different conceptual settings. On the one hand, within the classical hypoelastic framework which does not have a thermodynamic law, e.g., Zbib and Aifantis [5], Fleck and Hutchinson [6], Zbib [7]. Related to this type of material formulation Sluys et al. [8], de Borst et al. [9,10], and Pamin [11] have proposed numerical algorithms for the stress integrations at the local and finite element level.

On the other hand, gradient-dependent material formulations were analyzed and advocated within a thermodynamic framework, e.g., Valanis [12], Dillon and Kratochvil [13], and more recently Valanis [14] and Svedberg and Runesson [15]. In this last case the nonlocal character of the constitutive equations is restricted to the internal variables, leading to an additive expression of the free energy density.

A detailed discussion regarding the different gradient models of plasticity is given in Fleck and Hutchinson [16,17] and where the subtle differences in regularizing softening and in introducing size effects is highlighted.

In this work, the localization properties of the thermodynamically consistent gradient-dependent J_2 plasticity model with isotropic hardening/softening law are analyzed by means of the geometrical method.

To this end, the gradient-dependent elastoplastic localization properties are cast in the form of an elliptical envelope condition in the $\sigma_N - \tau_N$ coordinates of Mohr, see Pijaudier-Cabot and Benallal [18], Liebe and Willam [19]. Therefore, the tangency condition between the localization ellipse and the major principal circle defines the existence of localized failure mode and the corresponding critical directions. In the present analysis, the geometrical localization condition is defined in terms of the degree of nonlocality of the constitutive model that in case of gradient plasticity is represented by the characteristic length.

2 Gradient-Dependent Elastoplasticity

We follow the thermodynamically consistent gradient-dependent material theory by Svedberg and Runesson [15]. After reviewing the relevant thermodynamic and constitutive equations, the J_2 gradient elastoplastic model is presented, in which the nonlocal character is restricted to the internal plastic variables.

2.1 Thermodynamic Consistency. Under consideration of small strain kinematics, the free energy density of a strain gradient elastoplastic continuum can be expressed in an additive form as

$$\rho\Psi(\boldsymbol{\varepsilon}^e,\kappa,\nabla\kappa) = \rho\Psi^e(\boldsymbol{\varepsilon}^e) + \rho\Psi^{p,\mathrm{loc}}(\kappa) + \rho\Psi^{p,g}(\nabla\kappa) \tag{1}$$

where ρ is the material density. The elastic free energy density is defined as $\rho\Psi^e(\boldsymbol{\varepsilon}^e)=(1/2)\boldsymbol{\varepsilon}^e:\mathbb{E}^e:\boldsymbol{\varepsilon}^e$, $\boldsymbol{\varepsilon}^e$ and $\mathbb{E}^e$ being the elastic strain tensor and the fourth-order elastic operator, respectively.

The local and gradient free energy density contributions due to inelastic strains $\Psi^{p,\mathrm{loc}}$ and $\Psi^{p,g}$ are expressed in terms of the scalar hardening/softening variable κ. We observe in Eq. (1) that the gradient effects are only restricted to hardening/softening behavior via the inclusion of $\nabla\kappa$.

From the Coleman's relations follow the constitutive equations

$$\boldsymbol{\sigma} = \rho\frac{\partial\Psi}{\partial\boldsymbol{\varepsilon}} \quad \boldsymbol{\sigma} = \mathbb{E}^e:\boldsymbol{\varepsilon}^e \tag{2}$$

whereby $\boldsymbol{\sigma}$ is the stress tensor and $\boldsymbol{\varepsilon}$ the strain tensor. The dissipative stress within the continuum is defined as

$$K = K^{\mathrm{loc}} + K^g \tag{3}$$

being

$$K^{\mathrm{loc}} = -\rho\frac{\partial\Psi^{p,\mathrm{loc}}}{\partial\kappa} \quad K^g = \nabla\cdot\left(\rho\frac{\partial\Psi^{p,g}}{\partial(\nabla\kappa)}\right) \tag{4}$$

while on the boundary $\partial\Omega$, the dissipative stress due to the gradient in the second equation in Eq. (4) turns

$$K^{(g,b)} = -\mathbf{m}\cdot\rho\frac{\partial\Psi^{p,g}}{\partial(\nabla\kappa)} \tag{5}$$

with the (outward) normal $\mathbf{m}$ to $\partial\Omega$.

2.2 Constitutive Equations

2.2.1 General Case. Considering a convex set B of plastically admissible states defined as $B=\{(\boldsymbol{\sigma},K)\,|\,\Phi(\boldsymbol{\sigma},K)\leq 0\}$ with the convex yield function $\Phi=\Phi(\boldsymbol{\sigma},K)$, and a dissipative potential $\Phi^*=\Phi^*(\boldsymbol{\sigma},K)$, which turns Φ in case of associated plasticity. Then, the rate equations for the inelastic strains $\dot{\boldsymbol{\varepsilon}}^p$ and the scalar hardening/softening variable $\dot{\kappa}$, take the forms

$$\dot{\boldsymbol{\varepsilon}}^p = \dot{\lambda}\frac{\partial\Phi^*}{\partial\boldsymbol{\sigma}} \quad \text{and} \quad \dot{\kappa} = \dot{\lambda}\frac{\partial\Phi^*}{\partial K} \tag{6}$$

where $\dot{\lambda}$ is the rate of the plastic parameter.

From the Prandtl-Reuss additive decomposition of the total strain rate tensor into the elastic and plastic components that characterized the flow theory of plasticity and considering Eqs. (2), (4), and (6) follow the constitutive equations (in rate form)

$$\dot{\boldsymbol{\sigma}} = \dot{\boldsymbol{\sigma}}^e - \dot{\lambda}\mathbb{E}^e\frac{\partial\Phi^*}{\partial\boldsymbol{\sigma}} \quad \text{with} \quad \dot{\boldsymbol{\sigma}}^e = \mathbb{E}^e:\dot{\boldsymbol{\varepsilon}} \tag{7}$$

$$\dot{K}^{\mathrm{loc}} = -\dot{\lambda}\mathbf{H}\frac{\partial\Phi^*}{\partial K} \tag{8}$$

and

$$\dot{K}^g = l^2\nabla\cdot\mathbf{H}^g\cdot\left[\nabla\dot{\lambda}\frac{\partial\Phi^*}{\partial K} + \dot{\lambda}\nabla K\frac{\partial^2\Phi^*}{\partial K^2}\right] \tag{9}$$

which on the boundary turns

$$\dot{K}^{(g,b)} = -l^2\mathbf{m}\cdot\mathbf{H}^g\cdot\left[\nabla\dot{\lambda}\frac{\partial\Phi^*}{\partial K} + \dot{\lambda}\nabla K\frac{\partial^2\Phi^*}{\partial K^2}\right] \tag{10}$$

In the above equations, two types of state parameters were considered. On the one hand, the *local* hardening/softening modulus H and, on the other hand, the second-order tensor of *nonlocal gradient* state parameters $\mathbf{H}^g$ defined as

$$\mathbf{H}^g = \rho\frac{1}{l^2}\frac{\partial^2\Psi^{p,g}}{\partial(\nabla\kappa)\otimes\partial(\nabla\kappa)} \tag{11}$$

with

$$\det(\mathbf{H}^g)\geq 0 \tag{12}$$

As pointed out by Svedberg and Runesson [15], there are three possible interpretations for the characteristic length l in Eq. (11): as a convenient dimensional parameter which allows that both H and $\mathbf{H}^g$ get the same dimension, as a physical entity that defines the characteristic measure of the microstructure, and as a parameter that brings numerical stabilization to the local constitutive theory.

The Kuhn-Tucker conditions complete the rate formulation of the gradient-dependent plasticity in terms of hardening variables which, similar to the local theory, are defined by

$$\dot{\lambda}\geq 0 \quad \Phi(\boldsymbol{\sigma},K)\leq 0 \quad \dot{\lambda}\Phi(\boldsymbol{\sigma},K)=0 \tag{13}$$

2.2.2 J_2 Material Model. The expression of the von Mises yield criterium, corresponding to J_2 materials, yields

$$\Phi(\boldsymbol{\sigma},K) = \sigma_e - \sigma_y - K \quad \sigma_e = \sqrt{\frac{3}{2}}|\mathbf{s}| \tag{14}$$

with σ_y the yield stress, K the dissipative stress and $\mathbf{s}$ the deviatoric stress tensor

$$\mathbf{s} = \boldsymbol{\sigma} - \mathbf{I}\sigma_0 \quad \text{with} \quad \sigma_0 = \frac{\sigma_{ii}}{3} \quad \text{and} \quad i=1,2,3 \tag{15}$$

$\mathbf{I}$ being the second-order identity tensor.

The flow and hardening rules are of the associative type, therefore the rate equations for the internal variables in Eq. (6) are

$$\dot{\boldsymbol{\varepsilon}}^p = \dot{\lambda}\frac{3\mathbf{s}}{2\sigma_e} \quad \text{and} \quad \dot{\kappa} = -\dot{\lambda} \tag{16}$$

The explicit expression of the dissipative stress K in Eq. (14) follows from Eqs. (3) and (4), where the local and gradient free energy densities take the forms

$$\rho\Psi^{p,\mathrm{loc}} = \tfrac{1}{2}H\kappa^2 \tag{17}$$

$$\rho\Psi^{p,g} = \frac{1}{2}l^2\,\nabla\kappa\cdot\mathbf{H}^g\cdot\nabla\kappa \tag{18}$$

Therefore, the components K^{loc} and K^g of K result now

$$K^{\mathrm{loc}} = -H\kappa \tag{19}$$

$$K^g = l^2\nabla\cdot(\mathbf{H}^g\cdot\nabla\kappa) \tag{20}$$

3 Condition for Localized Failure

From the continuum mechanic's viewpoint, localized failure modes are related to discontinuous bifurcations of the equilibrium path, and lead to the loss of ellipticity of the equations that govern the static equilibrium problem.

The inhomogeneous or localized deformation field exhibits a plane of discontinuity that can be identified by the singularity condition of the acoustic or localization second-order tensor, see Ottosen and Runesson [20] and Willam and Etse [21].

Local and gradient flow theories of plasticity both result in the tangential equation that reads

$$\dot{\boldsymbol{\sigma}} = \mathbb{E}^{ep}:\dot{\boldsymbol{\varepsilon}} \tag{21}$$

where $\mathbb{E}^{ep}$ denotes the elastoplastic material operator that can be expressed by means of the encompassing equation

$$\mathbb{E}^{ep} = \mathbb{E}^e - \frac{1}{(h+h_g)}\mathbb{E}^e:\frac{\partial\Phi^*}{\partial\boldsymbol{\sigma}}\otimes\frac{\partial\Phi}{\partial\boldsymbol{\sigma}}:\mathbb{E}^e \tag{22}$$

with the *local* and *nonlocal* generalized plastic moduli

$$h = \frac{\partial\Phi}{\partial\boldsymbol{\sigma}}:\mathbb{E}^e:\frac{\partial\Phi^*}{\partial\boldsymbol{\sigma}} + \bar{H} \tag{23}$$

and

Contributed by the Applied Mechanics Division of ASME for publication in the JOURNAL OF APPLIED MECHANICS. Manuscript received September 21, 2005; final manuscript received April 6, 2006. Review conducted by G. C. Buscaglia. Discussion on the paper should be addressed to the Editor, Prof. Robert M. McMeeking, Journal of Applied Machanics, Department of Mechanical and Environmental Engineering, University of California–Santa Barbara, Santa Barbara, CA 93106-5070, and will be accepted until four months after final publication of the paper itself in the ASME JOURNAL OF APPLIED MECHANICS.

$$h^g = \begin{cases} 0 & \text{for local plasticity} \\ \mathbf{n}_l \cdot \bar{\mathbf{H}}^g \cdot \mathbf{n}_l \left(\dfrac{2\pi l}{\delta}\right)^2 & \text{for gradient-dependent plasticity} \end{cases} \tag{24}$$

δ being the width of the localization zone, $\mathbf{n}_l$ the normal direction to the discontinuous surfaces, and

$$\bar{H} = H \frac{\partial \Phi}{\partial K} \frac{\partial \Phi^*}{\partial K} \tag{25}$$

$$\bar{\mathbf{H}}^g = \mathbf{H}^g \frac{\partial \Phi}{\partial K} \frac{\partial \Phi^*}{\partial K} \tag{26}$$

From Eq. (26) and for the particular case of gradient isotropy, we obtain

$$\bar{\mathbf{H}}^g = \bar{H}^g \mathbf{I} \tag{27}$$

with $\bar{H}^g$ a positive, nonzero scalar. As $\mathbf{n}_l$ is a unit vector, results

$$\mathbf{n}_l \cdot \bar{\mathbf{H}}^g \cdot \mathbf{n}_l = \bar{H}^g \tag{28}$$

and, from the second equation in Eq. (24)

$$h^g = \bar{H}^g \left(\frac{2\pi l}{\delta}\right)^2 \tag{29}$$

In case of localized failure forms associated with discontinuous bifurcation we resort to the gradient elastoplastic localization tensor defined as

$$\mathbf{Q}^{epg} = \mathbf{Q}^e - \frac{1}{h + h^g} \mathbf{a}^* \otimes \mathbf{a} \tag{30}$$

with the elastic-localization tensor

$$\mathbf{Q}^e = \mathbf{n}_l \cdot \mathbf{E}^e \cdot \mathbf{n}_l \tag{31}$$

and

$$\mathbf{a}^* = \frac{\partial \Phi^*}{\partial \boldsymbol{\sigma}} : \mathbf{E}^e \cdot \mathbf{n}_l \tag{32}$$

$$\mathbf{a} = \frac{\partial \Phi}{\partial \boldsymbol{\sigma}} : \mathbf{E}^e \cdot \mathbf{n}_l \tag{33}$$

The localized failure condition in case of gradient-dependent elastoplasticity

$$\det(\mathbf{Q}^{epg}) = 0 \tag{34}$$

leads to the analysis of the spectral properties of $\mathbf{Q}^{epg}$. Its smallest eigenvalue, with respect to the metric defined by $\mathbf{Q}^e$, has the expression

$$\lambda^{(1)} = 1 - \frac{\mathbf{a}(\mathbf{n}_l) \cdot [\mathbf{Q}^e(\mathbf{n}_l)]^{-1} \cdot \mathbf{a}^*(\mathbf{n}_l)}{h + h^g} = 0 \tag{35}$$

In case of gradient isotropy, the explicit form of Eq. (35) is

$$\mathcal{H} + \frac{\partial \Phi}{\partial \boldsymbol{\sigma}} : \mathbf{E}^e : \frac{\partial \Phi^*}{\partial \boldsymbol{\sigma}} - \mathbf{a} \cdot [\mathbf{Q}^e]^{-1} \cdot \mathbf{a}^* = 0 \tag{36}$$

with

$$\mathcal{H} = \bar{H}_c^g \left(\frac{2\pi l}{\delta}\right)^2 + \bar{H}_c \tag{37}$$

The localization condition in Eq. (36) serves as a basis for analytical and numerical evaluations of the localization directions $\mathbf{n}_l$ and of the corresponding graphical maximum hardening/softening parameters $\bar{H}_c(\mathbf{n}_l) = \max[\bar{H}(\mathbf{n}_l)]$ in case of local plasticity, and $\bar{H}_c^g(\mathbf{n}_l) = \max[\bar{H}^g(\mathbf{n}_l)]$ in gradient-dependent plasticity.

4 Geometrical Localization Analysis

In this section, the geometrical method for localization analysis is derived for the thermodynamically consistent gradient-dependent J_2 elastoplastic model formulation detailed in Sec. 2.2.2. The approach is based on the original proposal by Benallal [22], which was further developed by Pijaudier-Cabot and Benallal [18] and Liebe and Willam [19] for classical plasticity.

Equation (36) defines an ellipse in the $\sigma_N - \tau_N$ coordinates of Mohr

$$\sigma_N = \mathbf{n}_l \cdot \boldsymbol{\sigma} \cdot \mathbf{n}_l \quad s = \mathbf{n}_l \cdot \mathbf{s} \cdot \mathbf{n}_l \tag{38}$$

$$\tau_N^2 = (\mathbf{n}_l \cdot \mathbf{s}) \cdot (\mathbf{n}_l \cdot \mathbf{s}) - (\mathbf{n}_l \cdot \mathbf{s} \cdot \mathbf{n}_l)^2 \tag{39}$$

The critical direction $\mathbf{n}_l$, normal to the plane where the Mohr components are evaluated, and the maximum hardening/softening parameters $\bar{H}_c$ and $\bar{H}_c^g$ for localization are obtained when the Mohr circle of stresses

$$(\sigma_N - \sigma_c)^2 + \tau_N^2 = R^2 \tag{40}$$

contacts the elliptical localization envelope

$$\frac{(\sigma_N - \sigma_0)^2}{A^2} - \frac{\tau_N^2}{B^2} = 1 \tag{41}$$

where the center and radius of the Mohr circle, Eq. (40), are

$$\sigma_c = \frac{\sigma_1 + \sigma_3}{2} \tag{42}$$

and

$$R = \frac{\sigma_1 - \sigma_3}{2} \tag{43}$$

with σ_1 and σ_3, the major and minor principal stresses, respectively, and the center σ_0 and half axes A and B of the localization ellipse are defined in the following.

5 Localization Properties of J_2 Gradient-Dependent Elastoplasticity

Considering for the elastic tensor $\mathbf{E}^e$ the expression

$$\mathbf{E}^e = 2G\mathbf{I}_4 + \Lambda \mathbf{I} \otimes \mathbf{I} \tag{44}$$

with the shear module G and the Lamé's constant Λ, the traction vectors in Eqs. (32) and (33) can then be rewritten as

$$\mathbf{a}^* = \mathbf{a} = 2G\mathbf{n}_l \cdot \mathbf{s} \tag{45}$$

and from Eq. (31), the inverse of the localization tensor $\mathbb{Q}^e$ shields

$$[\mathbf{Q}^e]^{-1} = \frac{1}{G}\left[\mathbf{I} - \frac{1}{2(1-\nu)} \mathbf{n}_l \otimes \mathbf{n}_l\right] \tag{46}$$

with the Poisson's modulus ν. Replacing Eq. (46) in Eq. (36), and combining with Eqs. (38) and (39), the center σ_0 and the half axes A and B of the localization ellipse, Eq. (41), results

$$\sigma_0 = \tfrac{1}{3} I_1 \tag{47}$$

$$B^2 = J_2 \left(\frac{\mathcal{H}}{G} + 1\right) \tag{48}$$

$$A^2 = 2\frac{1-\nu}{1-2\nu} B^2 \tag{49}$$

In the particular case of classical elastoplasticity the inhomogeneous differential Eq. (36) turns

$$\bar{H}_c = -\frac{\partial \Phi}{\partial \boldsymbol{\sigma}} : \mathbf{E}^e : \frac{\partial \Phi^*}{\partial \boldsymbol{\sigma}} + \mathbf{a} \cdot [\mathbf{Q}^e]^{-1} \cdot \mathbf{a}^* \tag{50}$$

therefore, the parameter B^2 representing the vertical axis of the ellipse in Eq. (41) now takes now the form

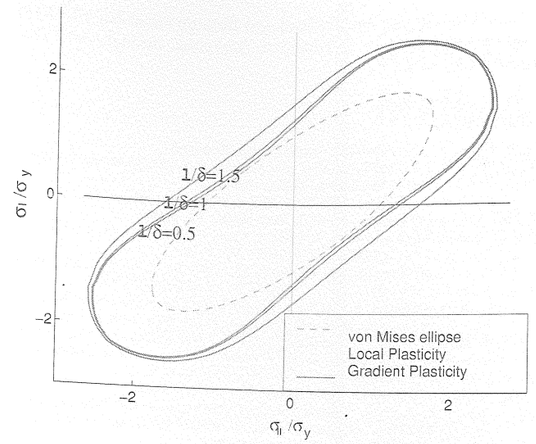

Fig. 1 Localization in local and gradient von Mises yield criterion in the principal stress space

$$B^2 = J_2 \left(\frac{\bar{H}_c}{G} + 1\right) \tag{51}$$

So, the thermodynamically consistent gradient-dependent plasticity formulation allows a simple extension of the geometrical localization method as demonstrated in this section. Thereby, the nonlocal effects in terms of the characteristic length and of the gradient hardening/softening modulus only affect the expression of the localization ellipse half axes A and B.

5.1 Graphical Analysis. The localization properties of the thermodynamically consistent gradient-dependent J_2 elastoplastic model are analyzed for the plane strain condition when $\sigma_z = \nu(\sigma_x + \sigma_y)$ and $\bar{H} = \bar{H}_c$, $\bar{H}$ being the particular hardening/softening modulus of the gradient-dependent model and $\bar{H}_c$ the critical one for localization of the local elastoplastic model. As follows from Eqs. (41), (48), and (37), the localization properties of the gradient-dependent J_2 elastoplastic model depend on the ratio δ/l. As the purpose of this work is to evaluate the performance of the condition for localized failure of the model by means of the geometrical method and not the calibration of the model, the analysis in this section will mainly focus on the sensitivity of the localized failure indicator performance regarding the variation of the ratio δ/l but not on the evaluation of the most appropriate value of this ratio for different types of metals.

The results in terms of $\det(\mathbb{Q})$ are depicted in Fig. 1 in the principal stress space. The adopted internal material length equals the width of the localization zone $l = \delta$. As can be observed in Fig. 1, the gradient-regularized plasticity is able to suppress the fulfilment of the localization condition, i.e., discontinuous bifurcation, for the whole range of limit stress states of the von Mises material, in the plane strain regime.

The geometrical localization analysis of the nonlocal gradient J_2 material formulation is performed for the simple shear, uniaxial compression, and uniaxial tensile tests and the results are shown on the left side of Figs. 2–4, respectively. These results illustrate the influence of the characteristic length l in the mode of failure. When $l > 0$, no contact is observed between the localization ellipses of the gradient-dependent plasticity model and the Mohr circle corresponding to the analyzed limit stress state. Thus, diffuse failure mode takes place for all three limit stress states. However, as $l/\delta \to 0$ the gradient-based localization ellipses approaches that of the local model which contacts the Mohr circle, indicating that the localization condition is fulfilled and therefore, discontinuous bifurcation takes place.

To verify the previous geometrical results regarding the capacity of the J_2 gradient-dependent model to suppress discontinuous bifurcations of the related local model formulation, a numerical localization study is performed at the constitutive level. The diagrams in the right side of Figs. 2–4 show the variation of the normalized localization indicator $\det(\mathbb{Q}^{epg})/\det(\mathbb{Q}^e)$ with the in-plane failure angles at peak of the pure shear, uniaxial compression, and tensile test, respectively. Both the local and the no-local gradient J_2 test are considered. These results demonstrate the capabilities of the J_2 gradient-dependent elastoplastic model formulation to eliminate discontinuous bifurcation in the form of localized failure.

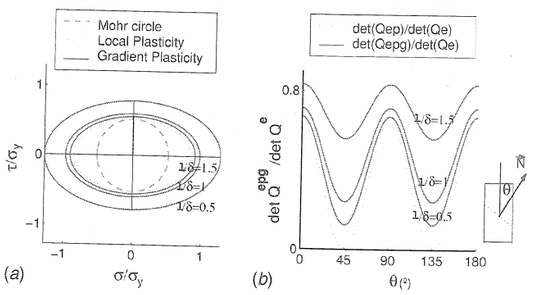

Fig. 2 Geometric and localization analysis at peak of the simple shear test. Local and gradient-dependent plasticity. J_2 material model.

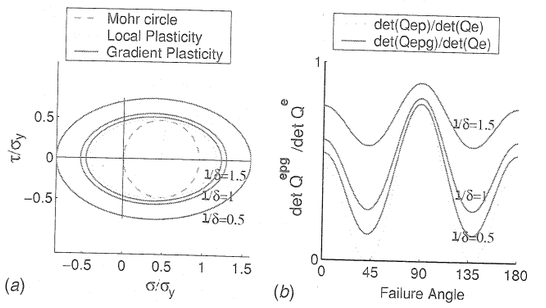

Fig. 4 Geometric localization analysis at peak of the uniaxial tensile test. Local and gradient-dependent plasticity. J_2 material model.

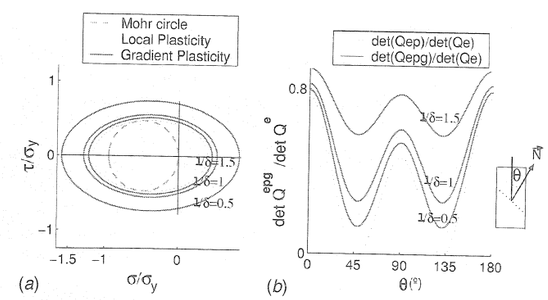

Fig. 3 Geometric localization analysis at peak of the uniaxial compression test. Local and gradient-dependent plasticity. J_2 material model.

6 Conclusions

In this work the geometrical localization method was extended for the analysis of the discontinuous bifurcation properties of the J_2 gradient-dependent elastoplasticity. The localization condition was expressed in terms of the coordinates of Mohr to obtain an ellipse that represents the envelope of localization for each particular state of stress. Thereby, localized failure mode is geometrically signalized by the tangency condition between the localization ellipse and the major principle circle of Mohr, while the critical localization direction is defined by the inclination of the Mohr circle radius to the tangential point with the localization ellipse.

The results of the geometrical localization analysis indicate that the J_2 gradient-dependent elastoplastic formulation suppresses the discontinuous bifurcations of the classical elastoplasticity when the selected hardening/softening modulus $\bar{H}$ equals the critical one for localization of the local material formulation $\bar{H}_c$.

The regularization capability of the gradient formulation reduces as $l/\delta \to 0$. Therefore, the characteristic length l defines the level of diffusion of the failure mode. When l approaches zero, a continuous transition from non-local gradient to local elastoplasticity is obtained. In the extreme case, when $l=0$, see Eqs. (37), (48), and (51), the local formulation is fully recovered.

Acknowledgment

The authors acknowledge the financial support for this work by FONCYT (Argentina Agency for the promotion of research and technology) through Grant No. PICT 12/9870 and by FUDETEC (Foundation for Technology Advancement). S.M.V. acknowledge the partial financial support to this work by CONICET (National Council for Science and Technology) through Grant No. PIP 3006 and by the University of Tucuman, Argentina, through Grant No. 26/E217.

References

[1] Nadai, A., 1931, *Plasticity*, McGraw-Hill, New York.
[2] Thomas, T., 1961, *Plastic Flow and Fracture in Solids*, Academic, London.
[3] Hill, R., 1962, J. Mech. Phys. Solids, **10**, p. 1.
[4] Rudnicki, J., and Rice, J., 1975, J. Engrg. Mech. Div., **23**, p. 371.
[5] Zbib, H., and Aifantis, E., 2002, Acta Mech., **92**, p. 209.
[6] Fleck, N., and Hutchinson, J., 1993, J. Mech. Phys. Solids, **41**, p. 1825.
[7] Zbib, H., 1994, ASME Mater. Instabil., **92**, p. 19.
[8] Sluys, L., de Borst, R., and Muhlhaus, M., 1993, Int. J. Solids Struct., **30**, p. 1153.
[9] de Borst, R., Pamin, J., and Sluys, L., 1995, *Continuum Models for Materials With Micro-Structure*, H. B. Muhlhaus, ed., Wiley, New York, p. 159.
[10] de Borst, R., Pamin, J., and Sluys, L., 1995, *Computational Plasticity, Fundamentals and Applications*, D. R. J. Owen, E. Onate, and E. Hinton, eds., Pineridge, Swansea, p. 509.
[11] Pamin, J., 1994, Ph.D. thesis, TU-Delft, The Netherlands.
[12] Valanis, K. C., 1968, "Unified Theory of Thermomechanical Behavior of Viscoplastic Materials," *Mechanical Behavior of Materials Under Dynamic Loads Symposium*, Springer, New York, pp. 343–364.
[13] Dillon, O., and Kratochvil, J., 1970, Int. J. Solids Struct., **6**, p. 1513.
[14] Valanis, K., 1998, Acta Mech., **127**, p. 1.
[15] Svedberg, T., and Runesson, K., 1997, Int. J. Plast., **13**, p. 669.
[16] Fleck, N., and Hutchinson, J., 1998, *Material Instabilities in Solids*, R. de Borst and E. van der Giessen eds., Wiley, New York, p. 507.
[17] Fleck, N., and Hutchinson, J., 2001, J. Mech. Phys. Solids, **49**, p. 2245.
[18] Pijaudier-Cabot, G., and Benallal, A., 1993, Int. J. Solids Struct., **30**, p. 1761.
[19] Liebe, T., and Willam, K., 2001, ASCE JEM, **127**(6), p. 616.
[20] Ottosen, N., and Runesson, K., 1991, Int. J. Solids Struct., **27**, p. 401.
[21] Willam, K., and Etse, G., 1990, "Failure Assessment of the Extended Leon Model for Plain Concrete," *Proceedings of Sci-C*, Second International Conference held at Zell am See, Austria, N. Bicanic and H. Mang, eds., Pineridge Press, Swansea, pp. 851–870.
[22] Benallal, A., 1992, Arch. Mech., **44**, p. 15.

Kinematic Laplacian Equation Method: A Velocity-Vorticity Formulation for the Navier-Stokes Equations

Fernando L. Ponta[1]
College of Engineering,
University of Buenos Aires,
Paseo Colón 850,
Buenos Aires C1063ACV,
Argentina
e-mail: fponta@fi.uba.ar

In this work, a novel procedure to solve the Navier-Stokes equations in the vorticity-velocity formulation is presented. The vorticity transport equation is solved as an ordinary differential equation (ODE) problem on each node of the spatial discretization. Evaluation of the right-hand side of the ODE system is computed from the spatial solution for the velocity field provided by a new partial differential equation expression called the kinematic Laplacian equation (KLE). This complete decoupling of the two variables in a vorticity-in-time/velocity-in-space split algorithm reduces the number of unknowns to solve in the time-integration process and also favors the use of advanced ODE algorithms, enhancing the efficiency and robustness of time integration. The issue of the imposition of vorticity boundary conditions is addressed, and details of the implementation of the KLE by isoparametric finite element discretization are given. Validation results of the KLE method applied to the study of the classical case of a circular cylinder in impulsive-started pure-translational steady motion are presented. The problem is solved at several Reynolds numbers in the range $5 < \mathrm{Re} < 180$ *comparing numerical results with experimental measurements and flow visualization plates. Finally, a recent result from a study on periodic vortex-array structures produced in the wake of forced-oscillating cylinders is included.* [DOI: 10.1115/1.2198245]

1 Introduction

During the last three decades several studies appeared concerning the representation of the Navier-Stokes equations in terms of non-primitive variables (namely the vorticity and the velocity potentials) instead of the classical formulation in terms of the primitive variables velocity and pressure. This family of approaches is generally known as vorticity-stream function $(\boldsymbol{\omega},\boldsymbol{\psi})$ methods. More recently, together with those works on the vorticity-stream function formulation and as a natural extension of them, a comparatively smaller number of studies were presented using a hybrid formulation in terms of the primitive and non-primitive variables velocity and vorticity. As several authors pointed out [1–3], the vorticity-velocity $(\boldsymbol{\omega},\boldsymbol{v})$ methods (as they are generally known) present some advantages compared with the classical formulation on primitive variables or with the vorticity-stream function methods, namely: (a) The pair of variables involved is particularly suited for a dynamic description of incompressible viscous flows. The vorticity is governed by a well understood dynamical equation while the velocity, which embodies the kinematical aspect of the problem, can be related to the vorticity by a simple elliptic equation. In vortex-dominated flows the vorticity advection is a fundamental process determining the dynamics of the flow, hence the vorticity-velocity description is closer to physical reality. (b) The variety of boundary conditions that can be chosen for the velocity potentials due to the nonuniqueness of the velocity representation is avoided since the velocity is supplemented by unique boundary conditions. (c) In some specific situations like that of external flows, boundary conditions at infinity are easier to implement for the vorticity than for the pressure. (d) The noninertial effects only enter the solution procedure of the $(\boldsymbol{\omega},\boldsymbol{v})$ formulation via the proper implementation of the initial and boundary conditions. Hence, the general applicability of an algorithm based on the $(\boldsymbol{\omega},\boldsymbol{v})$ formulation is enhanced because it is independent of whether or not the frame of reference is inertial.

The first uses of the $(\boldsymbol{\omega},\boldsymbol{v})$ formulation of the incompressible Navier-Stokes equations were reported by Fasel [4] who analyzed the stability of boundary layers in two dimensions and by Dennis, Ingham, and Cook [5] who derived a numerical method for computing steady-state three-dimensional flows. Both approaches were based on finite difference techniques. Since then several investigations have been conducted on incompressible hybrid variable models using variations of the finite difference approach (e.g., see [6–8], among others). A vorticity-velocity finite element solution of the three-dimensional compressible Navier-Stokes equations have been presented by Guevremont et al. [9] who investigated the steady state flow in a cubic cavity for several Mach numbers. More recently Clercx [2], then Davies and Carpenter [10], introduced pseudospectral procedures for the $(\boldsymbol{\omega},\boldsymbol{v})$ formulation. Lo and Young [11] presented an arbitrary Lagrangian-Eulerian $(\boldsymbol{\omega},\boldsymbol{v})$ method for two-dimensional free surface flow, using finite difference discretization for the free surface and finite element discretization for the interior of the domain.

A disadvantage of the vorticity-velocity formulation, compared with the formulation in primitive variables, is that in the most general three-dimensional case the $(\boldsymbol{\omega},\boldsymbol{v})$ formulation requires a total of six equations to be solved instead of the usual four of the primitive-variable approach [2]. The objective of the present study is to introduce a new method based on the $(\dot{\boldsymbol{\omega}},\boldsymbol{v})$ formulation which aims to tackle this six-unknown question and to improve some other aspects of the numerical implementation of the $(\boldsymbol{\omega},\boldsymbol{v})$

[1]Also at the Department of Theoretical and Applied Mechanics, University of Illinois at Urbana-Champaign, 104 S. Wright Street, Urbana, IL 61801.

Contributed by the Applied Mechanics Division of ASME for publication in the JOURNAL OF APPLIED MECHANICS. Manuscript received September 24, 2005; final manuscript received February 4, 2006. Review conducted by G. C. Buscaglia. Discussion on the paper should be addressed to the Editor, Prof. Robert M. McMeeking, Journal of Applied Mechanics, Department of Mechanical and Environmental Engineering, University of California – Santa Barbara, Santa Barbara, CA 93106-5070, and will be accepted until four months after final publication of the paper itself in the ASME JOURNAL OF APPLIED MECHANICS.

